Advanced Sensor Research

ADVANCED SENSOR RESEARCH Open Access

www.advsensorres.com

RESEARCH ARTICLE OPEN ACCESS

Smart Textile Based Wearable Sensors for Monitoring Isolation-Related Affective States: A Step Towards Loneliness Prediction

Jingqi Liu[1] | Freya Probst[2] | Yi Zhou[2] | John Ratcliffe[2] | Jessica Rees[3] | Erika Molteni[4] | Faith Matcham[5] | Sebastien Ourselin[4] | Michela Antonelli[4] | Anthea Tinker[3] | Wei Liu[2] | Yu Shi[1]

[1]School of Design, University of Leeds, Leeds, UK | [2]Department of Engineering, King's College London, London, UK | [3]Department of Global Health and Social Medicine, King's College London, London, UK | [4]School of Biomedical Engineering & Imaging Sciences, King's College London, London, UK | [5]School of Psychology, University of Sussex, Falmer, UK

Correspondence: Yu Shi (Y.Shi2@leeds.ac.uk)

Received: 13 October 2025 | **Revised:** 30 January 2026 | **Accepted:** 23 February 2026

Keywords: electrocardiography (ECG) | electromyography (EMG) | loneliness | mental health | physiological monitoring | respiration | skin conductance | smart textile | wearable technology

ABSTRACT

Loneliness is a significant psychosocial factor that negatively impacting the health and quality of life of individuals, with social isolation recognized as a major risk factor. This paper presents a wearable, textile based multi-sensing system to continuously monitoring physiological changes associated with isolation related affective states which toward future loneliness detection. The system integrates flexible, non-invasive textile sensors for electrocardiogram (ECG), electromyography (EMG), respiration, skin temperature, and galvanic skin response (GSR) within textile, enabling continuous physiological monitoring and analyses for analyzing loneliness resulting from isolation. In our pilot study, physiological signals are recorded dunder three controlled affective arousal conditions: Low emotional arousal induced by quiet sitting, moderate emotional arousal associated with social conversation, and high emotional arousal elicited by positive emotional arousal. Experimental results demonstrate distinct physiological patterns across conditions, including reduced heart rate variability, more regular respiration, lower skin conductance activity, and decreased muscular engagement under low emotional arousal compared with socially interactive and highly arousing states. This scalable and cost-effective solution supports proactive monitoring and assessment of loneliness for users, offering potential for timely interventions by caregivers, and clinicians. The work advances emotion-aware wearable systems for geriatric care and mental health support.

1 | Introduction

Loneliness is increasingly recognized as a critical risk factor for adverse health outcomes [1–6]. It could be linked to various physical ailments, such as cardiovascular diseases, diabetes, and weakened immune responses [7], and weakened immune functions [8], but also different mental health disorders, including depression [9], anxiety [10], and cognitive decline [11]. Research indicates that chronic loneliness may sustainably trigger the biological stress responses, elevating inflammation and thereby contributing to long-term morbidity and mortality risks [1, 12].

Traditional methods for diagnosing mental health, such as isolation and loneliness, primarily depend on self-reported questionnaires and interviews, which are inherently subjective, episodic, and prone to bias [7, 8, 13]. These tools often fail to capture the dynamic and physiological manifestations of emotional states [11, 14]. While self-report instruments offer useful subjective insights, they are insufficient for real-time detection and early prediction and intervention. Emotional experiences resulting from isolation and loneliness often trigger subtle physiological changes, such as fluctuations in heart rate, skin conductance, respiration etc. that unfold dynamically throughout the day [15, 16]. Therefore, such biological signals can be potentially used to monitor a dynamic emotional change due to isolation and loneliness by electrocardiogram (ECG) [17], respiration [18], galvanic skin response (GSR) [19], and sweat composition [20] sensors. Unlike self-reported measures of emotions, these biological signals could offer more reliable and objective data for predicting and diagnosing the mental health progress.

With advancements in wearable technology, there is a potential to shift toward objective, continuous monitoring [12] by the integrated wearable sensors, which can offer a continuous monitoring of the various physiological signals to enable a remote, reliable and timely early prediction and intervention by caregivers and clinic psychologists. A home-based digital solution for patients in management and rehabilitation of mental health conditions (isolation and loneliness) can be hence developed instead of appointments to visit psychological clinic [21]. Currently, there have been commercial wearable devices (e.g. smart watch), which have applied by clinicians for such purpose [22, 23]. However, these wearable devices would have to be worn on the wrist as the fixed location with integrated sensors, which the various physiological data could be limited with their accuracy. Smart watch is actually designed for the common application rather than a dedicated device for medical support, therefore, they also lack the specific sensing capabilities to detect key bioindicators for isolation and loneliness (e.g. GSR, sweat etc.).

Smart textiles with integrated electronics (or called "e-textiles") have attracted lots of studies in recent years due to their lightweight and ease to perform by users independently as different home products [24]. The various sensors integrated within textiles have shown huge potentials on health monitoring and diagnostics for home care and management, especially on mental health which may particularly require continuous bioindicators' measurement for emotional changes capturing and analyses. The key considerations and challenges in designing smart textiles extend beyond sensitivity and detection range to include comfort, integration methods, flexibility, and durability [25]. For instance, Danilo Pani et al. [26] introduced a textile electrode based on PEDOT:PSS, fabricated through an accessible soaking or screen printing method, which supports gel-free, comfortable ECG monitoring. These electrodes perform comparably to traditional gelled Ag/AgCl electrodes, offering stable, high quality recordings in both wet and dry conditions and demonstrating durable operation over 36 h of continuous usage which provide a compelling option for integration into smart garments [26]. Li et al. developed a breathable, skin-conformal humidity sensor capable of detecting emotional states such as fear, pain, and calm states [27]. However, the most work on wearables for healthcare were solely sensors focused research, which the data communication unit was ignored to demonstrate or was just simplified to utilise commercial hardware, such as Bluetooth [28] or RFID [29, 30] to prove the concept. But such technologies are less able to support a long range data transmission to support home-based data monitoring, especially which social carer or clinicians may need to remotely access to the data.

In addition, the smart textiles have been mostly reported for physiological health issues, such as musculoskeletal disorders, heart failure etc., there are limited research specifically addressing mental health, in particular, isolation and loneliness as this work concern.

Despite growing interest in physiological markers of loneliness and mental health, existing monitoring systems are often intrusive, clinic-bound, or unsuitable for long-term home use. There remains a critical need for a home-friendly, multimodal sensing platform that can unobtrusively capture physiological signals relevant to loneliness-related processes in everyday environments. To address this gap, this study proposes a multimodal physiological sensing textile platform designed for home-based mental health monitoring.

Therefore, in this work, a novel multi-sensor smart textile solution for long range remotely monitoring isolation and loneliness has been developed. We have identified the most relevant multi-sensors at co-design phase for ageing isolation and loneliness in previous study [31], in this work, we further optimally designed patterns of multi-sensors and integration within textile, combining the sensing capabilities for ECG, EMG, body temperature, respiratory, and GSR data measurements and analyses. The multi-physiological signals of individuals were collected to monitor the emotional changes resulted from isolation and induced loneliness. The embedment of these sensors on a textile will reduce any stress caused by systems for home monitoring such as cameras, which are considered more invasive [27]. The sensors are printed on stretchable TPU substrate and integrated into textile to achieve flexible and comfortability purpose to meet potential ageing users' perspectives in our co-design study [24]. A wireless data transmission system was designed to support long range data transmission by referring to Lora technology (5 km in urban area), maximizing the capacity of remote monitoring in real time. Our smart textile aims to improve useability and inclusivity for potential users with isolation and loneliness issues who live independently, which can be easily designed as home products, e.g. apparel or furnishing. The multi-sensor data sets can be fully used for monitoring of emotional changes associated with isolation and loneliness, but also more widely for other mental health challenges, such as anxiety and depression etc.

2 | Methods

2.1 | Design and Fabrication of Multi-Sensing Smart Textile and Smart Electronic System

Smart textile has been demonstrated lightweight, user and environmentally friendly, low cost, capable of degradation or decomposition and therefore has attracted huge research interest recently [32]. To monitor loneliness, a multi-physical sensing system was designed by integrating ECG, EMG, GSR, respiratory, and human body temperature sensors together to measure and analyze the various physiological signs of the users' activities. The integrated multi-sensors, shown in Figure 1, includes three multifunctional electrodes to measure ECG, EMG and GSR. The

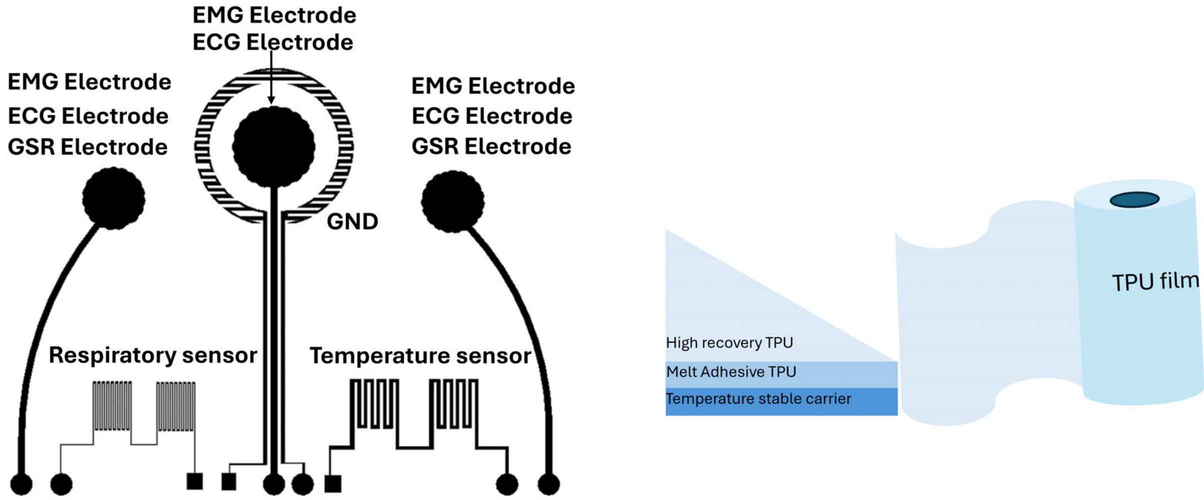

FIGURE 1 | Design of integrated multi-sensors' pattern structure of interfacial integration by TPU films.

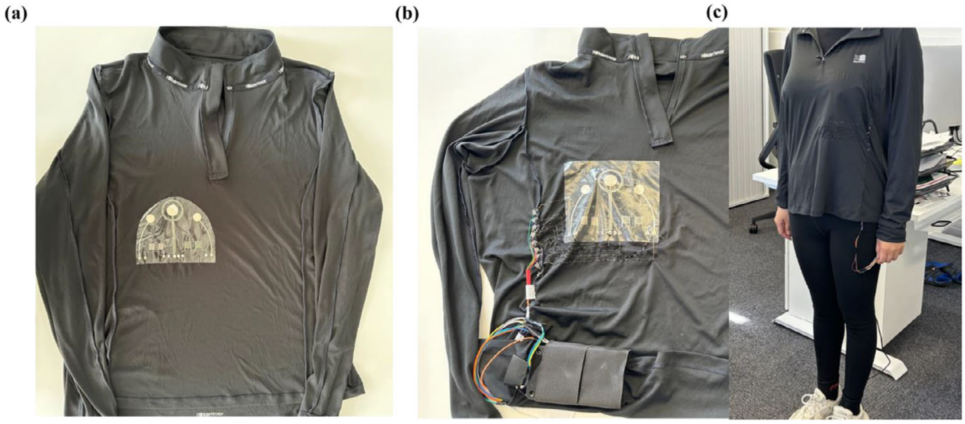

FIGURE 2 | Photograph of (a) integrated multi-sensors with encapsulation, (b) full connection and assembly of smart textile and (c) front view of wearing for testing.

respiratory and temperature sensors consist of two strain sensor arrays to capture the resistance change due to the breath induced stretching and temperature variations of the human body. The sensors were laminated on the T shirt placed under the chest area for measurements.

The comfortability for users with long-term wearing testing has been improved by the idea of using a 100% polyester Karrimor T shirt was chosen where the multi-sensors, were printed with stretchable electronic conductive silver inks (DYCOTE DM-SIP) onto a stretchable bilayer thermoplastic polyurethane (TPU, TE-11C) thin film due to reduced surface roughness and increased robustness of the sensors, as well as their biocompatibility with human skin. A melt adhesive layer was aplied for bonding to the fabrics under heat press lamination which enables screen printing for large area production.

The smart textile was integrated and encapsulated with TPU thin films, as shown by Figure 2a while a fully electronics assembly and connection for normal functionalization can be found in Figure 2b. The optimally designed multi-sensing pattern (Figure 1) was initially loaded into the screen mash and then printed onto the TPU substrate, and eventually laminated onto the textile by hot press at 120°C for 20 s for integration. The TPU substrate ensures a high-quality integration onto a rough and porous textile surface by hot press with minimum risks of debonding during daily wearing or washing. Screen printing is a highly efficient and low-cost method for future high volume and large-scale home textile products manufacturing, which the fabrication process of screen-printed sensor was shown in detail by Figure 3. By balancing the material stability and electrical performance, a curing temperature of 100°C for 10 min was exploited. The multi-sensors were sewed to the snapped button with conductive yarns which connects to the data acquisition circuit (Figure 2b). In Figure 2c, it demonstrates a fully integrated smart textile T shirt to be worn as their readiness for testing.

A wearable smart multi-sensing circuit system with long-range data communication capability was designed by referring to Lora techniques as they have been proven widely for long-range and low power communication and data transmission on remote monitoring while low power consumption. The NM180100 sys-

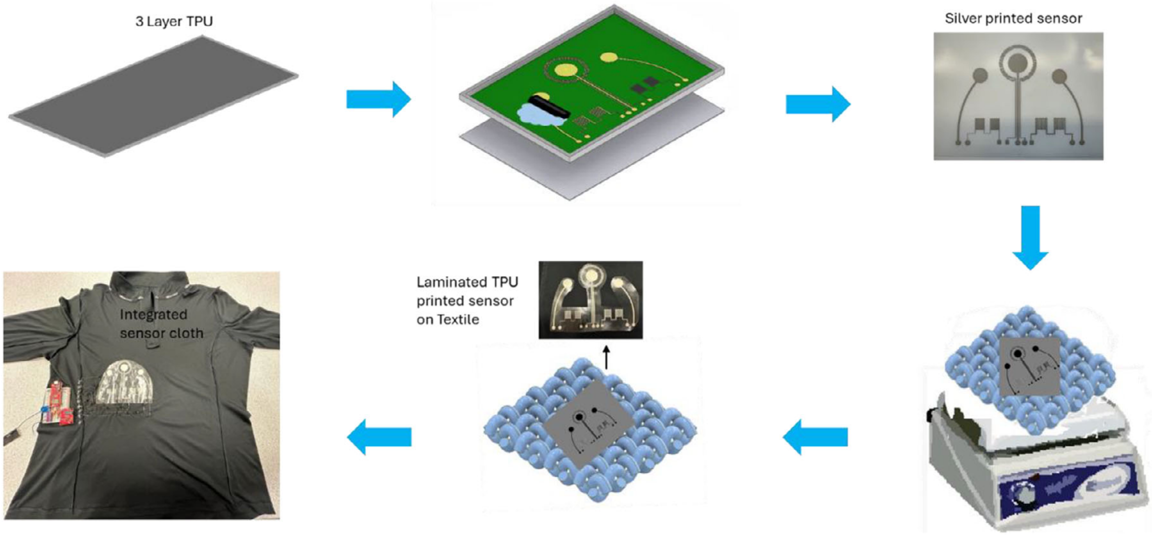

FIGURE 3 | Fabrication process of multi-sensors with textile.

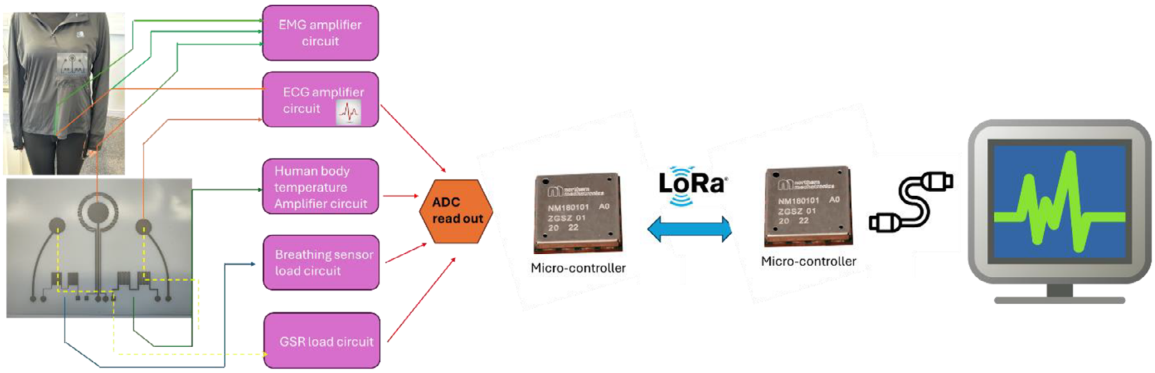

FIGURE 4 | Wearable health monitoring system schematic. This setup includes embedded sensors in clothing for ECG, EMG, human body temperature, breathing, and galvanic skin response (GSR) measurements. Signals from the ECG, EMG amplifier circuit, human body temperature amplifier circuit, breathing sensor lead circuit, and GSR load circuit are digitized using an ADC. A microcontroller transmits the data wirelessly via LoRa to another microcontroller, which then forwards the information to a computer for real-time display and analysis.

tem was selected to collect and control data transmission, combining with Apollo3 MCU and SX1262 LoRa module with FPU (up to 96 MHz), which could build the foundation of establishing an IoT system to remotely monitor multiple users at the same time.

The micro-controller Apollo3 in this work mainly gathers readings from the integrated human body temperature, ECG, EMG, GSR and respiration sensors' circuits system as shown in Figure 4. The respiration and human body temperature sensors have been designed based on measurement of the changes in resistance due to the deformation generated by breath and temperature variations. The temperature sensors were tested and measured using chip MAX30205 with a sensitivity of 0.1°C achieved at the temperature range from 25 to 45°C.

The screen-printed body temperature sensor was designed as a serpentine structure (Figure 1) which is commonly used in tracking resistance changes when external heat is applied. The active area is 1.1 cm × 1.7 cm with 2 sensor arrays connected, the serpentine path allows for mechanical changes in resistance which makes it suitable for sensing application.

Similarly, the resistive sensor layout to measure respiration was designed as a serpentine pattern, with 1.5 cm length and 1.2 cm width of each serpentine array. This pattern design was aimed to increase the sensing surface area while keeping the formal compact. Two electrodes on the bottom were connected to the signal processing circuit (Figure 1).

The ECG and EMG signals can be measured through the electrical impulses with variations of the heart beats and muscle reactions, respectively. The ECG and EMG sensors in this work were designed to jointly share three electrodes (Figure 1). The ECG measures the voltage difference between the right and left electrodes, and central electrode provides a reference point that helps in reducing common-mode noise (~50–60 Hz from the power line). This design helps to monitor heart rate, heart rate variability, and could reflect respiration rate. The smart textile EMG sensors have shared three electrodes with ECG sensors, shown as Figure 1, to track the dynamic response of motions by recording electrical activity of muscles.

The GSR sensor can capture the changes in skin's electrical properties due to sweat gland activity through designed electrodes, indicating emotional arousal, e.g. stress or excitement, as controlled by the autonomic nervous system. In this study, the designed GSR sensor consisted of two silver printed electrodes as shown in Figure 1.

The sensor converts these changes in resistance, conductance, and voltage into an electrical signal, and the amplifier is designed and used to view these changes. A filter then removes the amplified noise (details demonstrated in supporting document). The filtered signal is read by an analogue to digital converter in a microcontroller Apollo3 and transmitted through SX1262 LoRa module.

2.2 | Experimental Tests and Pilot Study

One major challenge to smart textile in commercial exploitation is its reduced performance after numerous washes. Research [33] has indicated that washing cycles could drastically reduce the electrical conductivity of smart textiles compared to the initial measurement, especially for non-encapsulated samples. One of the potential reasons is the delamination from mechanical stress induced by the washing process. Although the present study was motivated by theoretical models linking social isolation, loneliness, and physiological regulation, loneliness itself was not directly measured using a validated self-report instrument. Instead, the experimental manipulation targeted affective arousal states that may co-occur with or contribute to loneliness-related processes. As loneliness is a subjective and socially contextualized experience, future studies should incorporate direct psychometric assessments to more precisely map affective and physiological responses onto the construct of loneliness.

In this work, the washing tests were followed by ISO 6330 standard[34]at 40°C for 47 min with wash for non-encapsulated and encapsulated samples, respectively, and all samples were washed in 10 cycle times.

To perform a pilot study by assessing our smart textile for monitoring of isolation and loneliness, 10 participants (7 female and 3 male) were selected as adults aged between their 30 and 50 s, recruited through convenience sampling. All participants have provided informed consent prior to participating in the study with a full ethical review approved in advance by University of Leeds.

During the study, the participants wore the smart textile garment in a controlled office environment while physiological signals were continuously recorded using the integrated textile-based multi-sensors.

Three experimental scenarios were designed to help measure and collect the multi-physiological data for isolation and loneliness analyses by separating groups of participants with isolation and loneliness, and with social activities [35]. The details can be summarized as below.

To create an isolated and lonely group and testing environment, the participants were requested to quietly sit to wear the smart textile to continuously collect the multi-sensors data. Quiet sitting can minimize the confounding factors such as speech, movement, and social activities that influence physiological signals and analyses [36]. The absence of social and cognitive stimulation could correspond to a reduced sympathetic nervous system activity and lower emotional arousal (LEA) [37].

As comparison, a second group was designed to test the participants who wore the smart textile garment with social activities, showing the state of "moderate emotional arousal (MEA)". The MEA condition reflects a naturalistic social state by a casual conversation [38]. The participants in this group were requested to engage in a social conversation with other people during testing by introducing a moderate arousal state with subtle emotional changes.

To demonstrate how multi-sensors capability on emotional changes, a third group in experiment was introduced to build a strong comparison with isolation and loneliness by enthusiastic emotions, i.e. positive (joy) emotions. The participants were encouraged to laugh or maintain at a happy status with joyful emotion response by watching funny pictures from the GAPED Database, which is an official, licensed, database created by the University of Geneva for mental health related research [39]. This group with joyful states is defined as "high emotional arousal (HEA)" in our pilot study, aiming to elicit a strong and positive emotion response [40] to compare with LEA and MEA for smart textile analyses for isolation and loneliness monitoring.

Throughout the whole sessions, the multi-sensors data (respiration, EMG, ECG, GSR, and skin temperature) were continuously recorded by all participants for later analysis.

3 | Results and Discussion

3.1 | Body Temperature Sensor

The smart textile body temperature sensor was tested and validated by the commercial MAX30205 evaluation kit as shown in Figure 5a,b. The sensor was placed under the chest to monitor the temperature of the skin surface area. A comparison between smart textile sensors (black) and commercial sensors (red) in the range of 25–45°C has been shown in Figure 5c. The smart textile body temperature sensor has demonstrated a higher overall resistance around 7–24 Ω with an active area of 3.74 cm^2, which the commercial sensor was around 3–8 Ω with an active area of 0.49 cm^2. A higher sensitivity by our developed sensor was shown than commercial temperature sensor. The temperature coefficient of Resistance (TCR) was calculated by measuring the resistances values over an appropriate temperature range, (R2-R1)/R1(T2-T1). The TCR of smart textile sensor achieved 0.33 when measuring body temperature from 35 to 40°C while the TCR of commercial sensor was 0.25, which our smart textile sensor has shown a higher response from 35 to 40°C. Therefore, the smart textile body temperature sensor is proven with increased accuracy and sensitivity while being completely wearable and flexible for real-time monitoring.

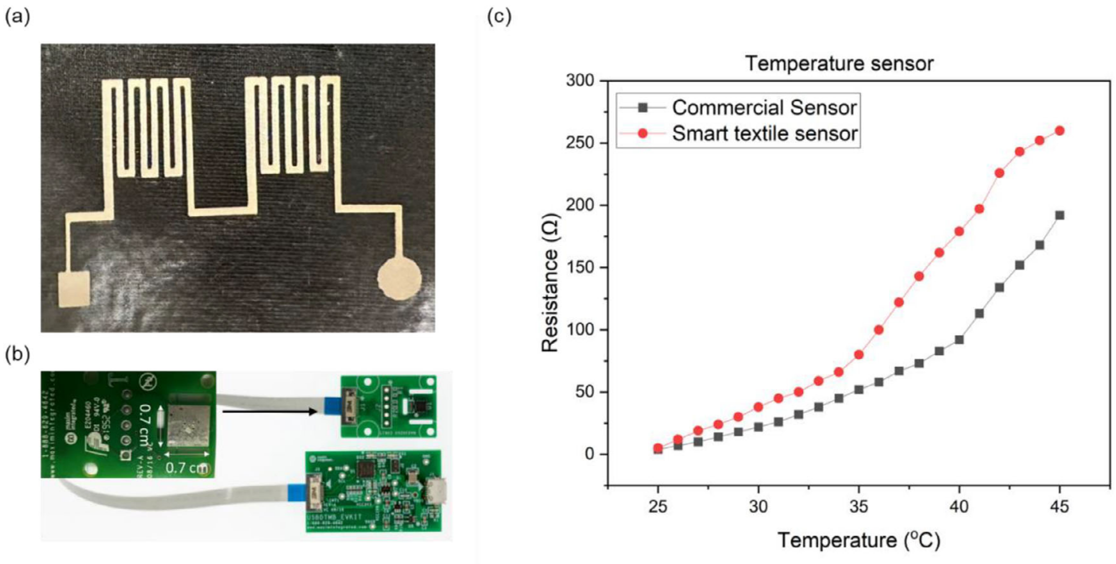

FIGURE 5 | (a) Photograph of smart textile human body temperature sensor, (b) commercial human body temperature sensor and (c) comparison of temperature changing between commercial and smart textile sensor.

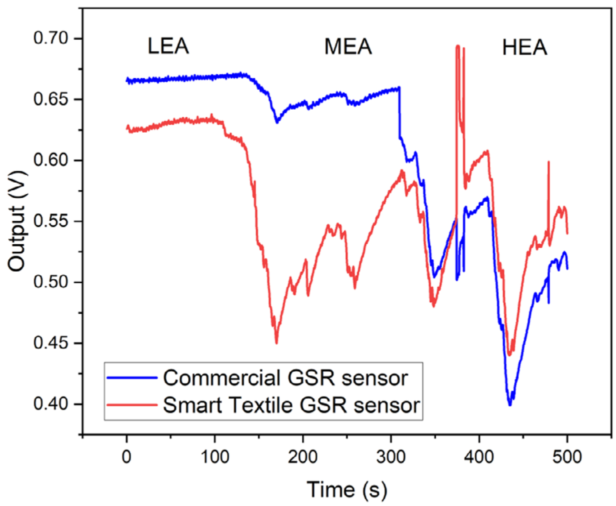

FIGURE 6 | GSR sensor testing on skin.

3.2 | Galvanic Skin Response Sensor

The galvanic skin responses have been successfully measured under three groups with different emotional states built. The developed smart textile Galvanic skin response (GSR) sensor was placed together in front of chest by contacting with the skin where the commercial electrodes were placed at the adjacent location of body to collect data for validation. The GSR signals from both smart textile-based sensor and the commercial reference sensor can be found in Figure 6, encompassing three distinct emotional arousal conditions: LEA, MEA, and HEA. The output voltage values were plotted against time (over a duration of 500 s) to visualize the physiological responses to different emotions' stimuli. The testing was carried out around 125 s in each status. There is a signal dropping or changing time around 50s between each emotional status. In Figure 6, it has shown that our smart textile GSR sensor has successfully tracked a consistent trend of the commercial sensor in all three groups with different emotional states.

During the LEA phase, both sensors exhibited stable signals with minimal fluctuation from 0–125 s. The commercial GSR sensor maintained a steady output around 0.66 V, while the smart textile GSR sensor recorded slightly lower readings, averaging approximately 0.62 V. The smart textile sensor signal started to drop slightly earlier than commercial sensor for around 25 s. During LEA, both sensors were highly stable, indicating that our textile sensor has demonstrated a strong reliability to measure the skin conductance (baseline) under the isolation and loneliness. The constant gap (around 0.4 V) of output voltage between two results was normal as what expected, which could be likely due to the difference in contact impedance between the textile material and the commercial electrodes.

Both sensors reached the lowest point at 175 s for reflecting to transit to another emotional status, MEA. In this situation, the smart textile sensor has exhibited a faster response and a more dramatic drop than commercial sensor when the low emotional arousal was broken. It well explained our textile GSR sensor has shown a better sensitivity to subtle changes. Although potential motion could be an alternative factor to lead to this drop, body movement and gestures are usually inevitable as part of social conversation together, which means the smart textile sensor indeed can more accurately reflect the emotional changes due to social conversations.

In the HEA phase, both sensors showed a sharp "valley", consistent with a spike in sympathetic nervous system activity. The smart textile sensor has recorded multiple sharp peaks, indicating the elevated skin conductance levels associated with heightened emotional states (e.g. excitement or joy). These peaks reflect the sensor's ability to capture rapid fluctuations in arousal varying levels.

Overall, both sensors showed a similar pattern and trend of skin conductance responses across the various emotional conditions, where the smart textile GSR sensor showed a higher degree of responsiveness and temporal detail.

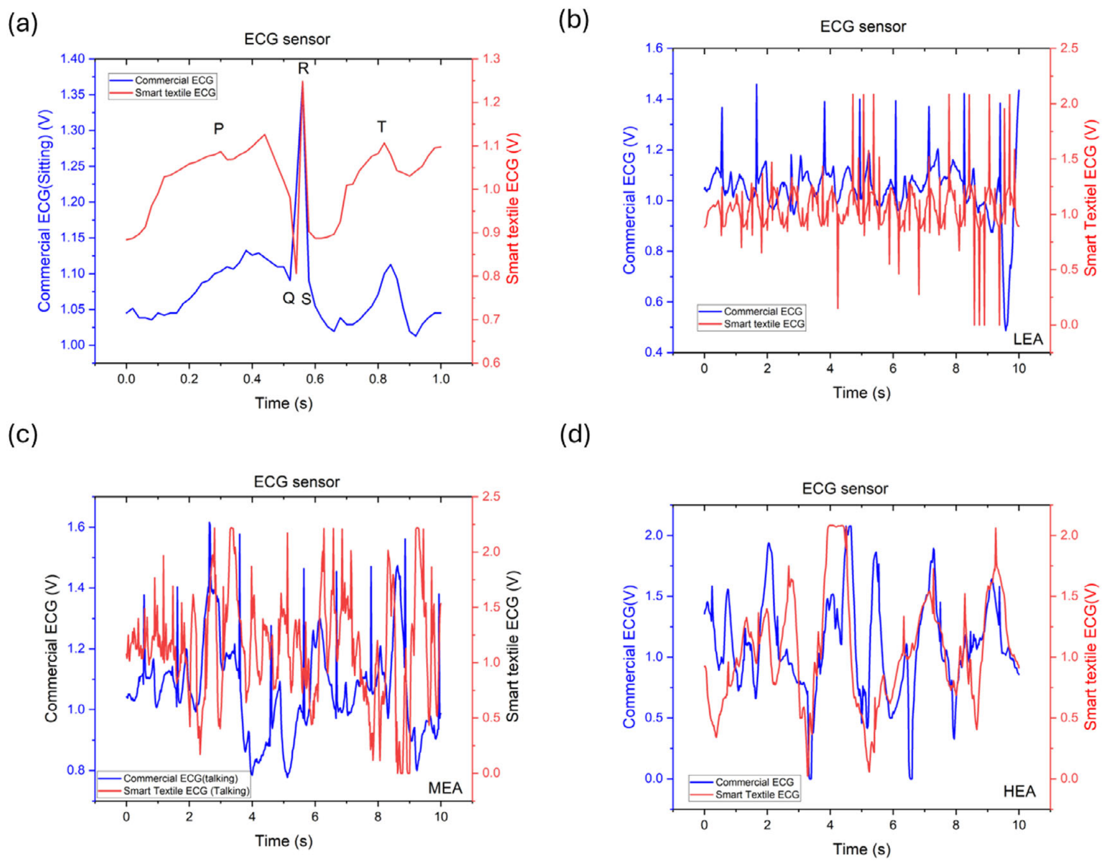

FIGURE 7 | Commercial ECG sensor and Smart textile ECG sensor in (a) low emotional arousal (lonely/isolated) condition, (b) single ECG signal, (c) moderate emotional arousal (normal social interaction) condition, and (d) high emotional arousal condition (laughter).

3.3 | Electrocardiogram Sensor

The smart textile three-electrode ECG sensors (Figure 1) were compared with commercial electrocardiogram (ECG) sensor, AD8232 evaluation kit, both of which were placed in front of the chest to ensure comparable electrode placement and physiological signal acquisition. Figure 7a–d represents a comparison of the ECG signals simultaneously recorded using the smart textile ECG sensor and the commercial ECG system under different conditions. A representative segment of a classic ECG curve was successfully captured by a magnified ECG segment over a second using our smart textile sensor comparing to commercial one by Figure 7a. Figure 7a clearly illustrated the P wave, QRS complex, and T wave captured by the smart textile ECG sensor. The timing of these waveform features closely matches that of the commercial ECG signal, confirming accurate temporal fidelity. Minor amplitude differences were observed, which would be within an expectation due to differences in electrode materials.

A 10-second period was chosen for LEA (Figure 7b), MEA (Figure 7c) and LEA (Figure 7d) conditions where shorter segments were used for clearer waveform illustration. Time intervals were selected because the observation of the remained data showing the similar and repetitive waveform patterns and therefore excluded.

In general, our smart textile ECG sensors have captured the reliable rhythmic timing of the heart's electrical activity for the heart rate (HR) and heart rate variability (HRV) analysis, across the three emotional arousal states, comparing with commercial sensors. When tested in the LEA condition (Figure 7a), both commercial and smart textile sensors tracked a highly overlapped periodic pattern, indicating a stability and accuracy of our smart textile sensors to measure ECG signals in the isolated and lonely emotion state. The heart rate remained steady as no emotional activity occurred with steady and regular signal patterns. However, the signal exhibited increased baseline fluctuations and higher susceptibility to transient noise, particularly during rapid voltage transitions such as the QRS complexes. These effects are attributed to the higher electrode skin impedance and less stable contact associated with a smaller effective electrode area. Despite these limitations, the smart textile ECG preserved accurate cardiac rhythm information, indicating its feasibility for basic heart rate monitoring.

In the MEA condition (Figure 7c), both sensors recorded increased heart rate and decreased regularity in waveform intervals compared to what measured under LEA, consistent with elevated autonomic activation. The output from the smart textile sensor displayed slightly higher amplitude fluctuation than the commercial reference, but retained a recognizable cardiac pattern aligned with the commercial signal in both frequency and timing. Such differences may be attributed in the motions produced by conversation.

During HEA testing (laughing and excitement), both sensors recorded pronounced variability in both amplitude and waveform shape which induced by such relatively intensive emotion state, as shown in Figure 7d. The smart textile sensor showed a greater dynamic range and responsiveness, with more frequent and higher peaks compared to the commercial sensor. However, the general waveform pattern and peak alignment between the two sensors remained consistent, indicating preserved temporal fidelity in detecting the cardiac signals for emotion prediction.

The smart textile ECG sensor demonstrated the ability to capture cardiac activities across the varying emotional arousal, with performance closely aligned to that of a commercially medical-grade ECG sensor. In particular, the signals tested under LEA scenario for isolation and loneliness, were nearly identical in morphology and timing, supporting the textile sensor's reliability in resting state detection. This consistency is essential for applications in continuous health monitoring where baseline tracking is crucial.

With changed emotional arousal at "simulated" non-lonely/isolated environments, physiological changes, such as elevated heart rate, greater sympathetic activity, and respiratory influence, introduced natural signal variability. The smart textile sensor captured these dynamic shifts effectively, exhibiting slightly higher sensitivity, as seen in the more pronounced peaks and broader amplitude ranges. This heightened responsiveness, especially at HEA condition, suggested that the smart textile sensor was more likely to be more reactive to subtle physiological fluctuations, possibly due to its flexible placement and conformable electrode-skin interface.

3.4 | Respiratory Sensor

To validate the smart textile respiration sensor, the commercial breathing belt was used as they have been mostly applied for clinic respiration measurement. Figure 8 presents the performance of the smart textile respiratory sensor under different arousal conditions, compared with a commercial breathing belt. Figure 8a shows the structure and layout of the fabricated textile respiratory sensor, while Figure 8b–d illustrate the simultaneously recorded respiratory signals under LEA, MEA and HEA conditions. Both sensors were placed together at the thoracic region to ensure consistent measurement of respiratory induced chest expansion. With a loop delay of 20 ms, the effective sampling rate of the respiratory sensor is approximately 50 Hz. It has to been noted that due to different outputs of smart textile respiration sensor (voltage) and breathing belt (pressure), the respiratory waveforms were mainly focused for validation in terms of breathing rate, temporal pattern, and cycles.

Under the LEA conditions as shown in Figure 8b, the smart textile respiratory sensor successfully captured periodic breathing cycles that correspond well with the commercial breathing belt signal. The temporal alignment between the peaks and troughs of the two signals confirms the detection of inhalation and exhalation phases. However, slight phase shifts and amplitude fluctuation are observed, which can be attributed to limited contact are and reduced mechanical coupling between the textile sensor and the body.

The differences between the smart textile respiratory sensor and the commercial breathing belt are mainly due to their different sensing methods. The breathing belt uses a differential air-pressure sensor to measure global thoracic volume changes and produces a smooth, conditioned signal, whereas the smart textile sensor responds to localized fabric strain and contact pressure, leading to a nonlinear and strain-dependent output. In addition, direct analogue acquisition without dedicated filtering makes the textile sensor more sensitive to motion artifacts and baseline fluctuations, resulting in differences in breathing cycle shape and timing.

In the MEA testing (Figure 8c) with social conversation introduced, the smart textile respiratory sensor exhibited a noticeable improvement in signal stability and consistency. The respiratory waveform showed a stronger agreement with the commercial breathing belt in terms of cycle timing and trend. The signal demonstrated reduced baseline variation and clearer peak definition, indicating enhanced sensitivity to chest movement. These results suggested improved mechanical interaction and strain transfer between the textile sensor and the body surface.

In HEA condition (Figure 8d), respiration rate became higher by smart textile sensor, consistently with heightened emotional arousal and positive affect. However, the belt pressure sensor seemed more erratic and irregular, which might be resulting from rapid and forceful contractions of chest due to laughing. This finding was helpful to identify our smart textile respiration sensor that may be more useful for clinic analysis as their waveform looks more regular on high emotional arousal scenarios that could results in intensive extraction of chest.

3.5 | EMG Sensor

The performance of the smart textile EMG sensor was benchmarked against the commercial Seeed Studio Grove EMG sensor, as illustrated in Figure 9, where the comparative EMG signal outputs from both sensors were shown at a 15 s interval for predefined three levels of emotional arousal, i.e. LEA, MEA, and HEA.

At LEA condition (Figure 9a), both smart textile and commercial EMG sensors maintained a stable baseline with similar voltage outputs (around 0.3 V). The EMG results aligned with the most other sensing results and findings that the muscles remained rest during quiet sitting (LEA). The good agreement between smart textile and commercial EMG sensors proves that the smart textile sensor could be sufficiently stable and reliable to monitor EMG signals when the user was stationary.

Under MEA condition (Figure 9b), as conversational activities dominated, both smart textile and commercial EMG sensors captured moderate, dynamic fluctuations in muscle activities. The smart textile sensor exhibited a more pronounced variations in amplitude compared to that measured under HEA condition, while maintaining general agreement with the commercial sensor in waveform shape and timing. The EMG sensor detected the muscle activity while talking produce wider variations on the output. The pronounced discrepancy between the commercial and smart textile EMG signals observed under moderate emotional arousal arises from the increased sensitivity of textile electrodes to motion artifacts and contact impedance variations during

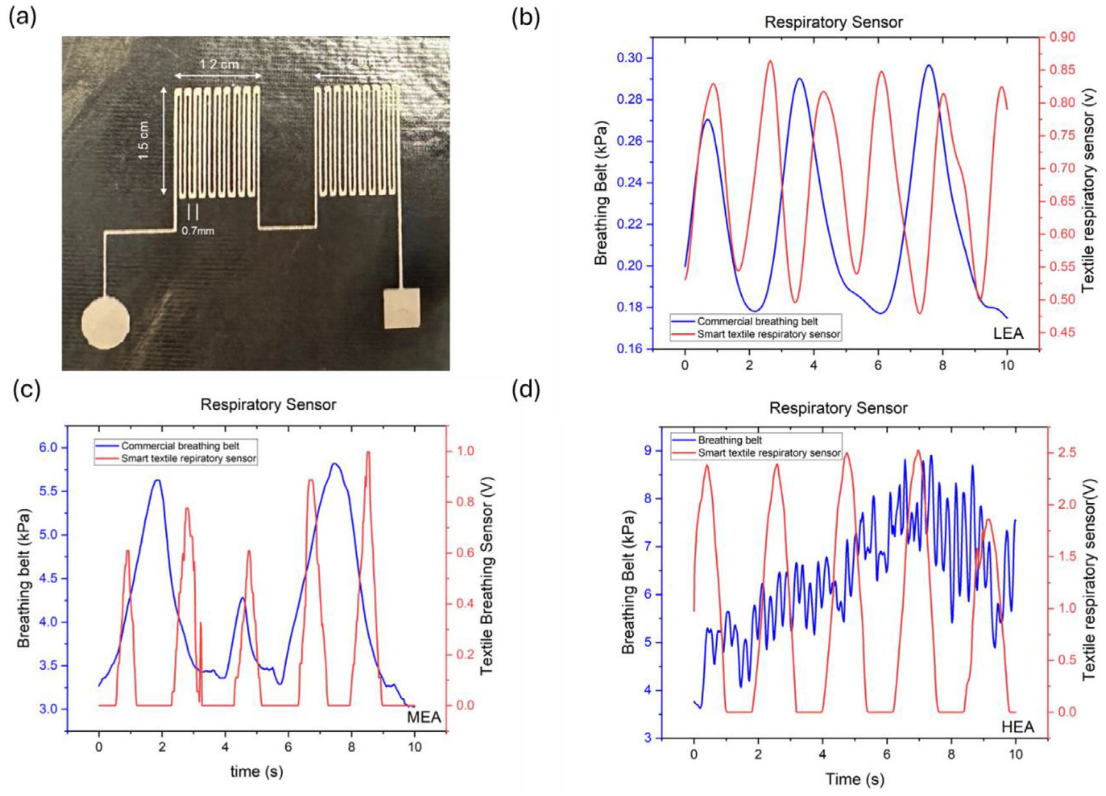

FIGURE 8 | Smart textile respiratory sensor validation with breathing belt, (a) photograph of respiratory sensor design (b) under LEA, and (c) under MEA, and (d) HEA.

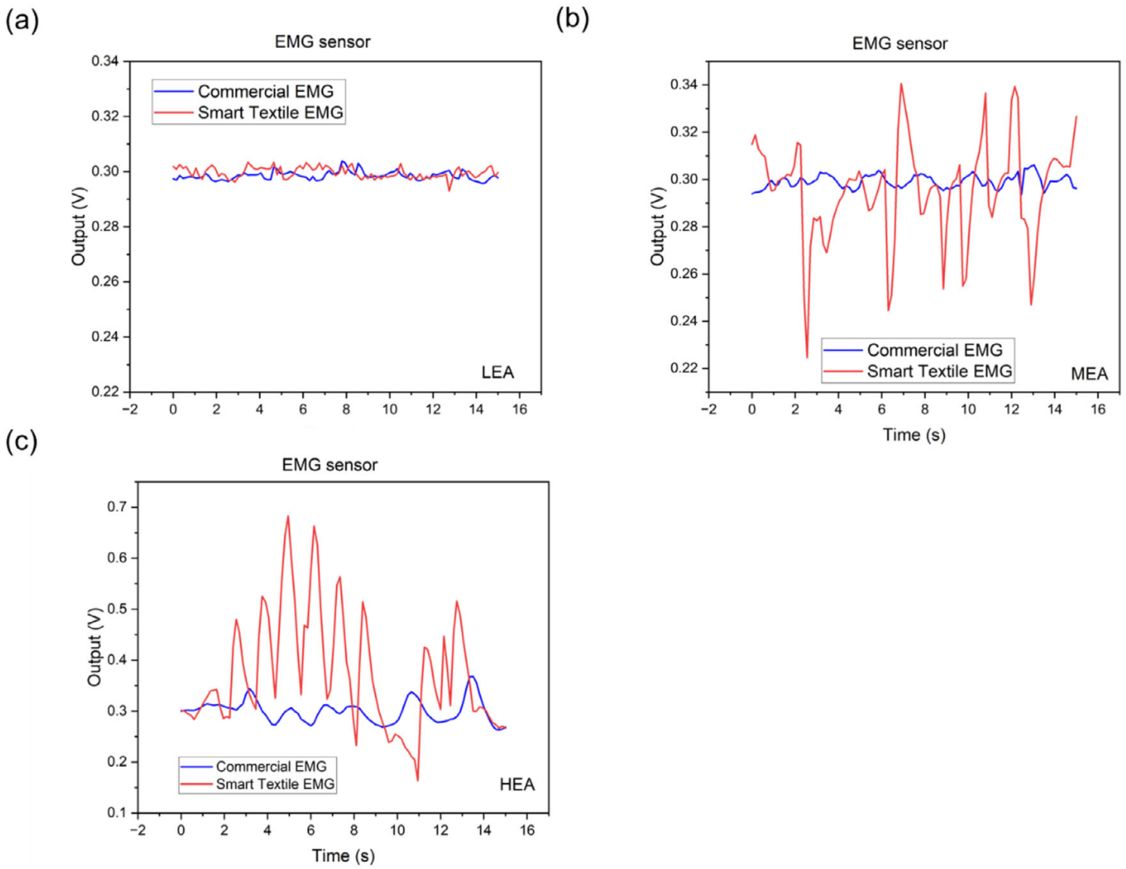

FIGURE 9 | Performance comparison between the smart textile EMG and commercial sensors in (a) low, (b) moderate, and (c) high emotional arousal.

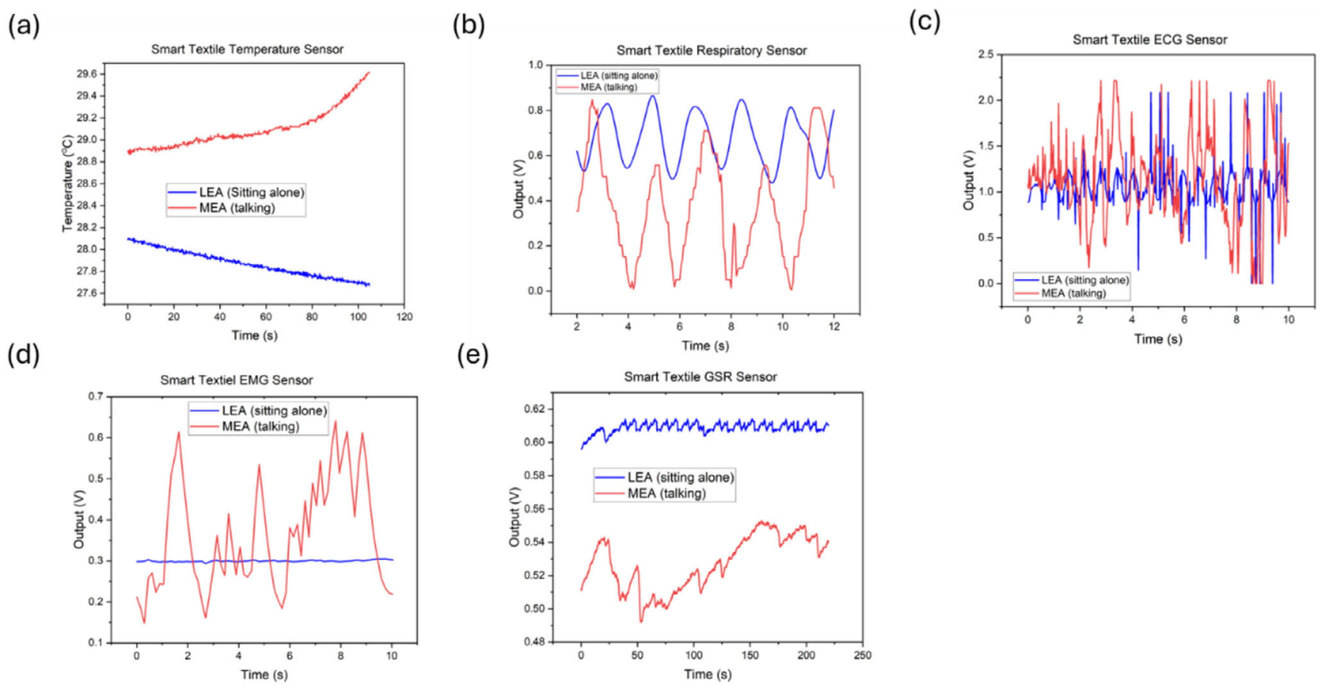

FIGURE 10 | Multiple sensor signal output under isolated and talking status, (a) temperature sensor,(b) breathing sensor,(c) ECG sensor, (d) EMG sensor and (e) GSR sensor.

subtle, intermittent muscle activity, whereas the commercial EMG system benefits from stable gel electrodes and integrated signal conditioning.

When tested at HEA state (Figure 9c), associated with laughing and excitement, both sensors showed clear and synchronous "bursts" (above 0.4 V) the smart textile EMG sensors reached a significantly higher amplitude peaks (~0.7 V). These brief but significant peaks correspond to muscle contractions triggered by high arousal and emotional reactivity. The signal returned to baseline following each spike, indicating good sensor recovery and baseline stability. It also indicated that our smart textile EMG sensor would be more sensitive at more intensive emotional response.

Collectively, the results suggest that the smart textile EMG sensor is not only effective for capturing voluntary muscle movement, but also well-suited for identifying emotion-related changes. This capability is valuable for affective computing, stress detection, and biofeedback interventions, where muscle responds to emotional changes.

3.6 | Emotional Assessment by Integrated Smart Textile Multi-Sensors

A synchronized output from multi-sensing system is shown in Figure 10, depicting the combined physiological signals' variations captured by smart textile sensors between LEA (isolated by sitting alone) and MEA (social communication with talking). The electronic system was linked to LoRa module to enable long distance wireless data transmission. To assess the remote monitoring, the pilot testing was performed by separating the participants from the receiver modules in different rooms within the building. The results demonstrated the module's capability to maintain stable connectivity over the tested distances. HEA condition wasn't considered for this combined study as it has been proved in previous section that obvious differences could be measured between LEA and MEA for emotional variation analysis.

In Figure 10a, the skin temperature changes between LEA and MEA conditions were measured by 2 min. A clear progressive change between the two conditions was observed over time. The temperature at LEA initiated from 28.1°C, gradually declining to approximately 27.7°C by the end of testing. This was highly possible due to a peripheral cooling for resulted lower skin temperature than human internal core temperature (around 36°C). The skin temperature was slightly decreased over the time of quiet sitting (LEA), which may be attributed in a lower metabolic rate or blood flow in such relaxed or low activation state. The temperature decline is smooth and stable, reflecting minimal movement and low sympathetic engagement.

On the other hand, the temperature at MEA condition started at 28.9°C and rose to 29.6°C by the end. Skin temperature showed a progressive increase over time, indicating an enhanced peripheral circulation associated with social interaction. This state may have triggered vasodilation and an increase in local metabolic activity, which elevated the skin temperature.

The observed temperature differences between LEA and MEA conditions align with established autonomic nervous system responses to emotional and social stimulation. Social interaction is known to modulate sympathetic and parasympathetic balance, influencing vasodilation and peripheral skin temperature. The smart textile sensor successfully captured these gradual thermal changes, demonstrating its sensitivity to emotion-related physiological modulation rather than a transient change.

The respiratory signals also varied between two conditions (Figure 10b), where a 10 s period data selected for analysis. The data reveal distinct patterns that highlighted breathing signal influences under these two conditions.

As shown in Figure 10b, under the LEA condition, the signal exhibits a regular and stable breathing pattern with consistent amplitude, indicating calm and controlled respiration. In contrast, during MEA (talking), the signal becomes more irregular with larger amplitude variations and sharper transitions, reflecting speech-related breathing, increased respiratory variability, and motion-induced changes in fabric strain. These results demonstrate that the smart textile respiratory sensor is sensitive to changes in breathing behavior associated with moderate emotional arousal, while also being influenced by body motion during talking.

ECG signals showed notable differences between these two conditions (Figure 10c), with similar 10 s interval results captured and compared. The notable differences in the amplitude and variability of the ECG signals could be observed under these two different states.

During LEA status, the ECG signal displays relatively stable amplitude and reduced variability, consistent with a calm physiological state. The waveform maintains identifiable cardiac activity with limited interference.

Under the MEA status condition, the ECG signal exhibits increased amplitude variation and higher signal fluctuations. These changes can be attributed to a combination of elevated heart rate, muscle activity, and motion artifacts introduced during speech. Despite the increased variability, the ECG signal retains recognizable cardiac patterns, demonstrating the robustness of the smart textile ECG sensor under moderate motion and arousal conditions.

In Figure 10d, the comparison of EMG signals over these two emotional conditions are demonstrated in with electrical progressive responses produced by skeletal muscles.

In LEA, the EMG output maintained relatively flat and stable, fluctuating narrowly around 0.3 V. The consistent signal meant a minimal muscle activation, which aligned with the scenario tested under silent sitting. No major spikes or dips were observed as there were no significant muscle movements.

Conversely, the EMG results measured under MEA condition with social conversations showed a more dynamic responsive pattern with sharp spikes, ranging from around 0.2 V to over 0.6 V. The amplitude was progressively increased from 4 to 8 s, aligning with the reality when more intensive or emotionally expressive speech at that time resulted in increased muscle engagement. It is worth to note that the EMG sensor demonstrated a “lag” to show the ending of speaking which was actually terminated after 6s. This would be due to potential recovery breath (or a deep exhale) to reset their breathing pattern to a resting state, which the physical reset could still be a final burst of chest muscles to last 1–2 s longer.

The contrast of EMG results between the two conditions clearly showed that talking (social activity) could generate a more dramatic EMG signal, whereas isolation and loneliness resulted in a flat baseline of muscle activity profile. Therefore, EMG would help emotional changes analysis where muscular patterns could provide insight into communication effort and intensity.

Similarly, GSR outputs were found with significant differences captured during LEA (sitting alone) and MEA (talking) conditions (Figure 10e). Differently from other four dataset, the GSR data recorded under a longer duration of 250 s was recorded as it took longer period to reflect a more obvious variation of sensed signs of skin conductance responses between LEA (isolation) and MEA (talking) conditions. The GSR during the isolated and lonely condition remained stable and flat, consistently around 0.6 V, suggesting low emotional reactivity in the absence of social communication. The GSR output starts at a lower level in MEA because the output drops when an activity occurs, it exhibits a gradual increasing trend and larger fluctuations over time, which are consistent with elevated sympathetic nervous system activity during talking. This confirms that the smart textile GSR sensor remains sensitive to arousal-induced changes.

Collectively, these findings supported the ability of our smart textile multi-sensing system to distinguish emotional changes for real-time mental health monitoring, stress tracking, and human-computer interaction for remote monitoring at home environment.

3.7 | Characterizations for Smart Textile Multi-Sensors

3.7.1 | Materials Characterization

A scanning electron microscopy was checked on both top and cross-section views of the developed sensors as shown in Figure 11. The sensor film morphology showed the nano particle size of silver printed silver of 25 nano meters with a thickness of 50 μm.

These layers suggested a deliberate deposition process, like Figure 11a showed the structure of the sensor. The bottom part with fiber shape is textile substrate and followed by a smooth layer is the TPU film, on top is the screen-printed silver. At higher magnifications (65 000 x and 100 000x), the surface is characterized by uniformly distributed nanostructures ranging from 14.49 to 26.95 nm in diameter. These nanoscale features indicated a high surface area, which explained the materials selected to benefit applications such as sensing.

3.7.2 | Washing Characterization

Figure 12 presents the washing durability of the ECG/EMG/GSR electrodes, temperature sensor, and respiratory sensor for both encapsulated and non-encapsulated samples, evaluated according to the ISO 6330 standard [34]. To enable comparison across

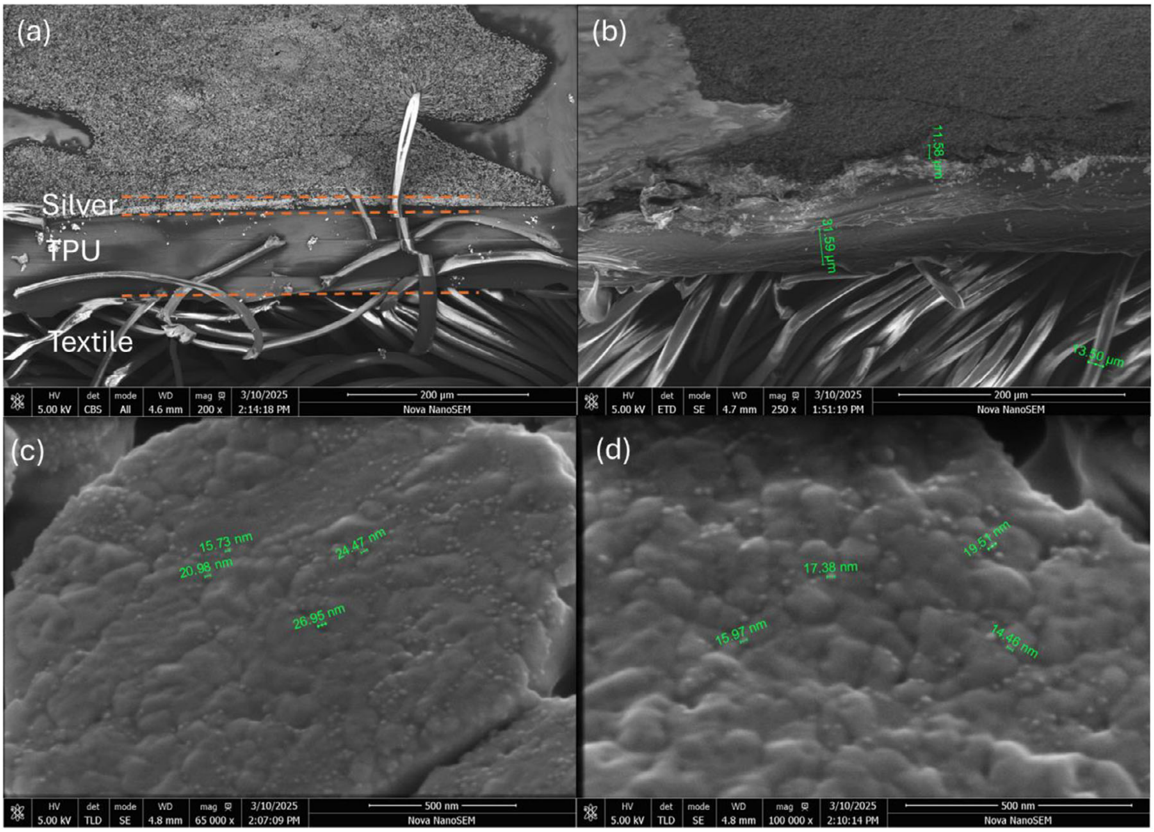

FIGURE 11 | (a,b)Cross-sectional view of the silver layer, (c)&(d) top view of the sensor in nano meter scale.

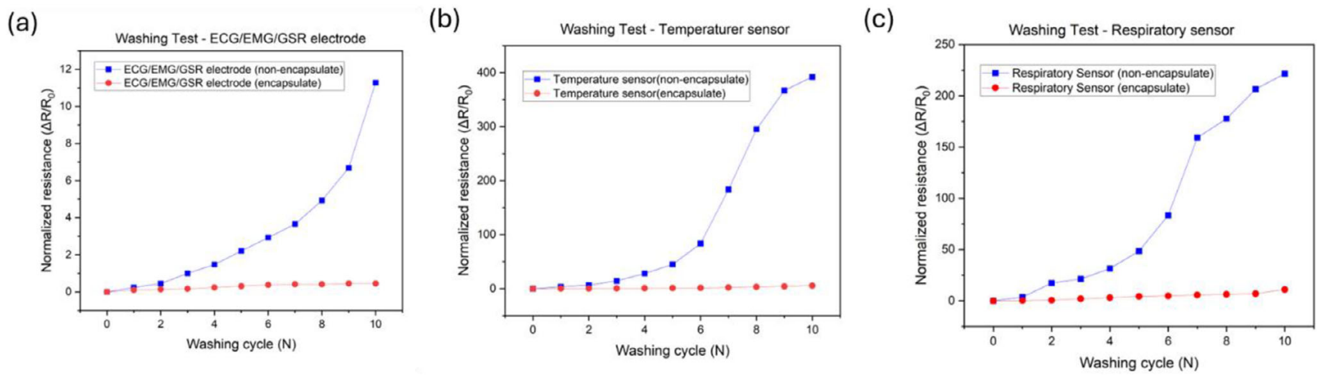

FIGURE 12 | Washing test results.

sensors with different initial resistance values and geometries, the results are presented as normalized resistance, calculated as $\Delta R/R_0$, where R_0 denotes the initial resistance prior to washing and ΔR represents the resistance change after each washing cycle.

For all sensor types, the non-encapsulated samples exhibited a rapid and pronounced increase in normalized resistance with increasing washing cycles. After the first few cycles, the resistance rose sharply, indicating significant degradation of the conductive pathways due to moisture ingress, detergent exposure, and mechanically induced delamination. This rapid increase in $\Delta R/R_0$ reflects severe loss of electrical integrity, suggesting that non-encapsulated sensors are unsuitable for repeated laundering in practical textile applications.

In contrast, the encapsulated sensors demonstrated substantially improved washing stability. Across up to ten washing cycles, the normalized resistance remained relatively low, with only gradual increases observed. This behavior indicates that encapsulation effectively protects the sensing elements from mechanical stress and environmental exposure during laundering. These results confirm that proper encapsulation is essential for enhancing the durability and long-term reliability of smart textile sensors intended for home and everyday use.

4 | Conclusions

This study presented a smart textile based multi-sensing system equipped with ECG, EMG, GSR, respiration, and human body temperature sensors, for continuous physiological monitoring in home environments. The individual textile sensors and integrated system were validated through comparison with commercial reference devices and demonstrated reliable performance across different affective arousal conditions

The integrated smart textile multi-sensing system was performed with pilot tests by our participants under two predefined emotional groups, i.e. low (isolation and loneliness) and moderate (social communication) emotional arousal conditions. The system captured district physiological patterns under low, moderate, and high emotional arousal states. In particular, the isolation related low arousal condition exhibited reduced heart rate variability, more regular respiration, lower skin conductance activity, and minimal muscular engagement when compared with socially interactive and highly arousing conditions. These findings indicate that the proposed smart textile platform can detect physiological signatures associated with affective states relevant to social isolation. The results provide foundational evidence that multimodal physiological sensing using smart textiles can capture isolation-related affective states that are theoretically and empirically linked to loneliness risk. This positions the proposed system as a meaningful step toward future loneliness monitoring frameworks when combined with validated psychological assessments and larger-scale longitudinal studies.

The platform further benefits from long-range wireless data transmission via LoRa technology, supporting remote and scalable monitoring in home settings. The use of screen-printing fabrication and encapsulation strategies demonstrates a pathway toward low-cost, durable, and manufacturable smart textile products suitable for everyday use.

Although multimodal data fusion combined with machine learning classifiers (e.g., SVM or Random Forest) is a promising approach for discriminating emotional states, such analyses require sufficiently large and diverse datasets to ensure reliable training and evaluation. In the present study, the limited number of participants and experimental duration preclude statistically robust machine learning modelling without substantial risk of overfitting. Therefore, the current work focuses on feature-level physiological analysis and within-subject statistical comparisons. Future studies will extend this framework by incorporating larger datasets to enable multimodal fusion and predictive modelling.

Overall, this work contributes an enabling wearable sensing technology for emotion-aware and mental healthcare monitoring. Future research will focus on expanding participant cohorts, incorporating validated loneliness measures, conducting robust statistical and longitudinal analyses, and exploring multimodal data fusion and predictive modelling. With these extensions, the proposed smart textile system has strong potential to support proactive mental health monitoring and early intervention strategies for populations at risk of social isolation and loneliness.

5 | Experimental Section

5.1 | Material

DuPont Intexar TE-11C was used as stretchable bilayer thermoplastic polyurethane (TPU) film. Screen printed silver paste from Dyetco. 100% polyester T-shirt from Karrimor. Screen mesh from MCI screen Ltd. Lora integrated board from Sparkfun.

5.2 | Fabrication Process

Silver paste was firstly screen printed onto the TE-11C TPU substrate. Trim the TPU to required size of the print after printing is completed. Remove the carrier layer of the TE-11C TPU substrate, and bond TE-11C to fabric cloth by laminating by hot press using a hot plate with temperature 125°C for 20 s. The pressure applied on the substrate was 420 kPa.

5.3 | Device Fabrication

The sensor pattern was initially designed in CAD software and transferred to a mesh screen. The silver conductive paste was screen-printed onto the TE-11C TPU substrate using a standard screen-printing process. After printing, the substrate was trimmed to the desired dimensions. The carrier layer of the TPU film was then removed, and the printed sensor film was laminated onto the polyester fabric using a hot-press lamination technique at a temperature of 125°C for 20 s under a pressure of 420 kPa.

Post-lamination, the samples were allowed to dry at room temperature for 15 min, followed by annealing in a convection oven at 100 °C for 10 min to enhance conductivity and adhesion. Metal snap buttons were sewn onto the T-shirt at the designated electrode connection points. Signal acquisition wires were subsequently connected to the snap buttons to interface the textile sensor with the external measurement circuitry.

5.4 | Sensor Integration and Electronics

The integrated sensor system was connected to a LoRa-enabled data acquisition board to facilitate long-range, wireless physiological signal transmission. The electrode layout and snap button connections were optimized for comfort, skin contact, and signal fidelity.

5.5 | SEM Scan

SEM imaging was conducted using the Nova NanoSEM 450 system to characterize the topography and cross-sectional morphology of the printed sensor. The surface structure and layer integrity were evaluated to ensure uniform conductivity and mechanical robustness of the printed traces.

5.6 | Washing Test

Washing tests were conducted in accordance with the ISO 6330 standard. The sample was first placed inside a protective laundry bag and then washed in a household washing machine together with 3 mL of liquid detergent. Each washing protocol consisted of a 47 min cycle, including washing, rinsing, and spinning, followed by 10 min of drying in a tumble dryer. The sample was subjected to a total of 10 consecutive washing and drying cycles. The resistance changing was captured after each washing cycle.

5.7 | Ethical Approval

FAHC 23–037 Amendment 1 – March 2025 – DEsign for healthy aging: a smart system to decrease LONELINESS for older people (DELONELINESS) was obtained from AHC Research ethics University of Leeds.

5.8 | Statistical Analysis

Physiological data from all sensors were acquired using the Arduino IDE and transmitted via the custom electronic system described above. Raw data streams were exported and further processed using Python for offline analysis. The sampling rate for each physiological modality (ECG, EMG, respiration, skin temperature, and GSR) followed the specifications described in the corresponding sensor sections.

5.9 | Data Pre-Processing

Given the pilot nature of this study and the limited sample size ($n = 10$), the statistical analysis focused on within-subject descriptive comparisons across emotional arousal conditions. Physiological signals were processed and analyzed in Python to extract representative features and trends under each condition. Data normality was not formally tested, and no inferential hypothesis testing was performed. Instead, differences between conditions were assessed descriptively using summary statistics (mean $\pm$ standard deviation) and visual inspection of signal patterns. This approach was adopted to explore physiological trends associated with different affective states while avoiding overinterpretation of statistical significance in a small exploratory dataset.

5.10 | Sample size

The pilot study included $n = 10$ participants, and all statistical analyses were conducted using within-subject comparisons across experimental conditions (low, moderate, and high emotional arousal). No between-group statistical analyses were performed.

5.11 | Software

All statistical analyses and data processing were performed using Python (including NumPy, SciPy, and Matplotlib libraries). Signal extraction and initial data acquisition were conducted using the Arduino IDE.

Acknowledgments

This work was supported by the EPSRC under Grant [number EP/W031442/2].

Funding

This work was supported by the EPSRC under Grant [number EP/W031442/2].

Conflicts of Interest

The authors declare no conflicts of interest.

Data Availability Statement

The data that support the findings of this study are available from the corresponding author upon reasonable request.

References

1. J. Holt-Lunstad, T. B. Smith, M. Baker, T. Harris, and D. Stephenson, "Loneliness and Social Isolation as Risk Factors for Mortality: A Meta-Analytic Review," *Perspectives on Psychological Science* 2 (2015): 10.

2. J. T. Cacioppo and S. Cacioppo, "Social Relationships and Health: The Toxic Effects of Perceived Social Isolation," *Social and Personality Psychology Compass* 8 (2014): 58–72.

3. T. N. A. Press. *Social Isolation and Loneliness in Older Adults: Opportunities for the Health Care System* (National Academies of Sciences, Engineering, and Medicine, 2020).

4. "The Hurt of Loneliness and Social Isolation," *Nature Mental Health* 2 (2024): 255–256.

5. K. Peternel, M. Pogacnik, R. Tavcar, and A. Kos, "Presence-Based Context-Aware Chronic Stress Recognition System," *Sensors* 12 (2012): 15888–15906.

6. R. N. Kann Holmén, R. N. Kjerstin Ericsson, L. Andersson, and B. Winblad, "Loneliness Among Elderly People Living in Stockholm: A Population Study," *Journal of advanced nursing* 17 (1992): 43–51.

7. D. W. Russell, "UCLA Loneliness Scale (Version 3): Reliability, Validity, and Factor Structure," *Journal of Personality Assessment* 66 (1996): 20–40.

8. T. Matthews, A. Danese, A. Caspi, et al., "Loneliness and Neighborhood Characteristics: A Multi-Informant, Nationally Representative Study of Young Adults," *Psychological Science* 30, no. 5 (2019): 765–775, https://doi.org/10.1177/0956797619836102.

9. T. Petitte, J. Mallow, E. Barnes, A. Petrone, T. Barr, and L. Theeke, "A Systematic Review of Loneliness and Common Chronic Physical Conditions in Adults," *The Open Psychology Journal* 8 (2015): 113–132.

10. P. Odriozola-González, A. Planchuelo-Gomez, M. J. Irurtia, and R. de Luis-García, "Psychological Effects of the COVID-19 Outbreak and Lockdown Among Students and Workers of a Spanish University," *Psychiatry Research* 290 (2020): 108–113.

11. J. T. Cacioppo and L. C. Hawkley, "Perceived Social Isolation and Cognition," *Trends in Cognitive Sciences* 13 (2009): 447–454.

12. L. C. Hawkley and J. T. Cacioppo, "Loneliness Matters: A Theoretical and Empirical Review of Consequences and Mechanisms," *Annals of Behavioral Medicine* 40 (2010): 218–227.

13. E. Van Roekel, M. Verhagen, R. C. M. E. Engels, R. H. J. Scholte, and J. T. Cacioppo, "Trait and State Levels of Loneliness in Early Adolescents: Examining the Role of Perceived Popularity," *Journal of Early Adolescence* 38 (2018): 69–91.

14. R. W. Picard, E. Vyzas, and J. Healey, "Toward Machine Emotional Intelligence: Analysis of Affective Physiological State," *IEEE Transactions on Pattern Analysis and Machine Intelligence* 23 (2001): 1175–1191.

15. M. Z. Poh, N. C. Swenson, and R. W. Picard, "A Wearable Sensor for Unobtrusive, Long-Term Assessment of Electrodermal Activity," *IEEE Transactions on Biomedical Engineering* 57 (2010): 1243–1252.

16. B. Reeder and A. David, "Health at Hand: A Systematic Review of Smart Watch Uses for Health and Wellness," *Journal of Biomedical Informatics* 63 (2016): 269–276.

17. J. Huang, Q. Wang, Q. C. Wang, et al., "Foundation models and intelligent decision-making: Progress, Challenges, and Perspectives," *Innovations* 6 (2025): 6.

18. Z. Yin, Y. Yang, C. Hu, J. Li, B. Qin, and X. Yang, "Wearable respiratory Sensors for Health Monitoring," *npg Asia Materials* 16 (2024): 8.

19. M. V. Villarejo, B. G. Zapirain, and A. M. Zorrilla, "A Stress Sensor Based on Galvanic Skin Response (GSR) Controlled by ZigBee," *Sensors* 12 (2012): 6075–6101.

20. S. Shanbhog M and J. Medikonda, "A Clinical and Technical Methodological Review on Stress Detection and Sleep Quality Prediction in an Academic Environment," *Computer Methods and Programs in Biomedicine* 235 (2023): 107521.

21. A. Alberdi, A. Aztiria, and A. Basarab, "Towards an Automatic Early Stress Recognition System for Office Environments Based on Multimodal Measurements: A Review," *Journal of Biomedical Informatics* 59 (2016): 49–75.

22. R. W. Picard, E. Vyzas, and J. Healey, "Emotion Measurement Using Wearable Sensors: New Possibilities in Affective Computing," *IEEE Computer* 49 (2016): 6.

23. P. Schmidt, A. Reiss, R. Duerichen, C. Marberger, and K. Van Laerhoven, "Introducing WESAD, a Multimodal Dataset for Wearable Stress and Affect Detection," in Proceedings of the 20th ACM International Conference on Multimodal Interaction 8 (2019), 436.

24. K. Cherenack and L. van Pieterson, "Smart Textiles: Challenges and Opportunities," *Journal of Applied Physics* 112 (2012): 091301.

25. L. M. Castano and A. B. Flatau, "Smart Fabric Sensors and E-Textile Technologies: A Review," *Smart Materials and Structures* 23 (2014): 053001.

26. A. Achilli, A. Bonfiglio, and D. Pani, "Design and characterization of screen-printed textile electrodes for ECG monitoring," *IEEE Sensors Journal* 18, no. 10 (2018): 4097–4107.

27. T. Li, H. Zhang, X. Zhao, and Z. Xu, "Skin-Conformal and Breathable Humidity Sensor for Emotional State Recognition," *ACS Applied Materials & Interfaces* 13 (2021): 2334–2345.

28. R. Tynan, "ZigBee Wireless Sensor Network Technology," *Electronics* 43 (2009): 4.

29. R. Colella and L. Catarinucci, "Wearable UHF RFID Sensor-Tag Based on Customized 3D-Printed Antenna Substrates," *IEEE Sensors Journal* 18, no.21 (2018): 8789–8795, https://doi.org/10.1109/JSEN.2018.2867597.

30. J. Yoo, "A 10.8 mW Body Area Network Transceiver With High Interference Immunity," *IEEE Journal of Solid-State Circuits* 44 (2009): 10.

31. F. Probst, J. Rees, Z. Aslam, et al., "Evaluating a Smart Textile Loneliness Monitoring System for Older People: Co-Design and Qualitative Focus Group Study," *JMIR Aging* 7 (2024): e57622.

32. M. Dulal, H. R. M. Modha, J. Liu, et al., "Sustainable, Wearable, and Eco-Friendly Electronic Textiles," *Energy & Environmental Materials* 8 (2024): e12854.

33. M. R. Islam, S. Afroj, C. Beach, et al., "Fully Printed and Multifunctional Graphene-Based Wearable E-Textiles for Personalized Healthcare Applications," *iScience* 25 (2022): 103945.

34. X. Guan, T. Lan, D. Zhao, et al., "Robust Textile-Based Electromagnetic Audio Interfaces," *Advanced Material* 38 (2025): e08022.

35. M. Cattan, M. White, J. Bond, and A. Learmouth, "Preventing Social Isolation and Loneliness Among Older People: A Systematic Review of Health Promotion Interventions," *Ageing and Society* 25 (2005): 41–67.

36. J. A. Healey and R. W. Picard, "Detecting Stress During Real-World Driving Tasks using Physiological Sensors," *IEEE Transactions on Intelligent Transportation Systems* 6 (2005): 156–166.

37. T.-V. T. Nguyen, R. M. Ryan, and E. L. Deci, "Solitude as an Approach to Affective Self-Regulation," *Personality and Social Psychology Bulletin* 44 (2017): 92–106.

38. S. W. Porges, "The Polyvagal Perspective," *Biological Psychology* 74 (2006): 116–143.

39. E. Dan-Glauser and K. R. Scherer, "The Geneva Affective Picture Database (GAPED): A New 730-picture Database Focusing on Valence and Normative Significance," *Behavior Research Methods* 43 (2011): 468.

40. M. Egger and S. Hanke, "Emotion Recognition From Physiological Signal Analysis: A Review," *Electronic Notes in Theoretical Computer Science* 343 (2019): 35–55.

Supporting Information

Additional supporting information can be found online in the Supporting Information section.

Supporting File: adsr70138-sup-0001-DataFile.xlsx